Available online at www.sciencedirect.com
ScienceDirect
International Journal of Multiphase Flow 33 (2007) 935–947
International Journal of Multiphase Flow
www.elsevier.com/locate/ijmulflow

Effect of temperature gradient on Marangoni condensation heat transfer for ethanol–water mixtures

Shen-Hua Hu, Jun-Jie Yan *, Jin-Shi Wang, Yang Li, Ji-Ping Liu

State Key Laboratory of Multiphase Flow in Power Engineering, Xi'an Jiaotong University, Xi'an 710049, PR China

Received 1 February 2007; received in revised form 27 March 2007

Abstract

This paper experimentally studied the effect of macroscopic temperature gradient on Marangoni condensation of ethanol–water vapor mixtures under a wide range of concentrations. For each concentration, the experiment was performed at different velocities and pressures. An oblique copper block was employed to create surface temperature gradient. The results indicated that local heat flux was varied along transversal condensation surface, which was caused by surface temperature gradient. This difference in heat flux might be attributed to the variation of condensate thickness on condensation surface. In addition, a mean heat transfer coefficient was derived along transversal condensation surface. For low ethanol concentration (0.5%, 1%), the coefficient kept a high value over a relative wide range of vapor-to-surface temperature difference (<10 K) and could be augmented as much as 15% as compared with literature under similar experimental condition. Moreover, the mean heat transfer coefficient generally increased with increasing velocity or pressure for all concentrations of the ethanol–water mixtures.
© 2007 Elsevier Ltd. All rights reserved.

Keywords: Condensation; Heat transfer; Oblique block; Temperature gradient; Marangoni effect

1. Introduction

The movements of liquids resulting from unbalanced surface tension constitute an important surface phenomenon, known as the Marangoni effect. The usual Marangoni effect is triggered by gradients in concentration (solutocapillary) or/and temperature (thermocapillary) on a liquid surface. In fact, the two effects usually coupled with each other and solutocapillary is generally much greater than thermocapillary. Marangoni effect can drive the liquid film condensate rise locally and create film instability, eventually form many drops on the film. Some researchers called it non-filmwise condensation, i.e., pseudo-dropwise condensation. Ford and Missen (1968) demonstrated that the criteria for film instability could be expressed simply by an inequality.

Marangoni effect can be achieved by introducing small amounts of heat transfer additives (ammonia, ethanol, etc.) into water to form binary or multi-component mixtures, and the literature devoted to the effect

* Corresponding author. Tel./fax: +86 29 8266 5741.
E-mail address: yanjj@mail.xjtu.edu.cn (J.-J. Yan).

0301-9322/$ - see front matter © 2007 Elsevier Ltd. All rights reserved.
doi:10.1016/j.ijmultiphaseflow.2007.03.005

was rich. Mirkovich and Missen (1961, 1963) firstly discovered non-filmwise condensation phenomenon of binary vapors and compared heat transfer coefficients of the various types of condensation of binary vapors. Morrison and Deans (1997) conducted an experiment that the ammonia water vapors flowing down a vertical duct were condensed on a short horizontal. Experimental studies of steam condensation to a bundle of horizontal tubes with small amounts of effective additives by Kim et al. (2001) were performed to evaluate their effect on condensation heat transfer and to identify the onset of heat transfer enhancement. Chris and Joe (2004) examined ammonia–water mixtures condensed in a horizontal shell and tube condenser. The researchers above all studied relation between ammonia concentration and heat transfer coefficient, and concluded that the heat transfer coefficient would be enhanced (13–30%) at low concentration due to Marangoni effect.

The heat transfer characteristics of ethanol–water mixtures was investigated by Utaka and Terachi (1995, 1996) and they found that surface vapor-to-surface temperature difference was the fundamental factor controlling the condensate form. Fujii et al. (1989, 1993) had presented an experimental study concerning condensation of water and ethanol mixtures on a horizontal tube. When ethanol vapor concentrations varied from 0%–20%, the heat transfer coefficient was less than that of pure steam. Hijikata et al. (1992) conducted an experiment of ethanol–water mixture condensation on a flat block, revealed that for vapor ethanol concentrations of 4–66%, the heat transfer coefficient was equal to or less than that of pure steam. Further, Hijikata et al. (1996) made the theoretical and experimental investigations for the condensation mechanisms of ethanol–water vapor mixture, and heat transfer coefficient were relatively low. On the other hand, Yan et al. (2007) studied the main influencing factors for Marangoni condensation of ethanol–water vapor on a flat block, and demonstrated that the heat transfer coefficient had a maximum value when the ethanol mass fraction was 1%. Utaka and Wang (2004) carried out a series of experiments on Marangoni condensation for ethanol–water vapor mixtures, and pointed out that the maximum heat transfer coefficients in the condensation characteristic curves appeared at an ethanol vapor mass fraction of approximately 1%. The condensation heat transfer was enhanced approximately 2–8 times compared to pure steam. Their findings were approximately consistent with the general findings of Chris and Joe (2004).

There was, however, little experiment concerning Marangoni effect with macroscopic temperature gradient. The condensation surface temperature mentioned above was uniform, regardless of experimental or theoretical research. Moreover, the experiments introduced earlier were performed under atmospheric or constant pressure. The objective of the present paper was to study the effect of temperature gradient on condensation heat transfer for ethanol–water mixtures vapor at various velocities and pressures.

2. Experimental apparatus

The experimental apparatus system as shown in Fig. 1 was made of a boiler, a test chamber, an auxiliary condenser, a vacuum pump, and water reservoir, etc. The boiler had a total heating capacity of 9 kW with a controller. The test chamber contained a sight glasses to observe and photograph the mode of condensation. To achieve high cooling intensities required, the rear side of the test block was cooled by jet cooling water. Pressure in test chamber was measured with a pressure sensor (MSI, accuracy 0.1%). Vapor temperature was measured with two thermocouples in the test chamber. The thermocouples and the pressure gauge were connected to a data acquisition system (NI), where the temperatures and pressure were monitored and stored. The whole system was tested for any leaks to minimize the detrimental effect of non-condensables in the condensation process.

The mixture was heated and vaporized from the boiler, and then the vapor was led into the upper entrance of test chamber, where the vapor partly condensed on the vertical surface of the test block. The remaining vapor condensed in the auxiliary condenser, and returned by gravity to the boiler along with condensate in the test chamber. Cooling water supplied from a water reservoir was heated very slowly, and pumped to the back of the test block. The vacuum pump with cooling water system kept working during the experiment to avoid the influence of non-condensable gas. The aperture of valve for vacuum pump was very small, so magnitude of extraction by vacuum pump was negligible. A constant pressure could achieve by adjusting cooling water valve of the condenser.

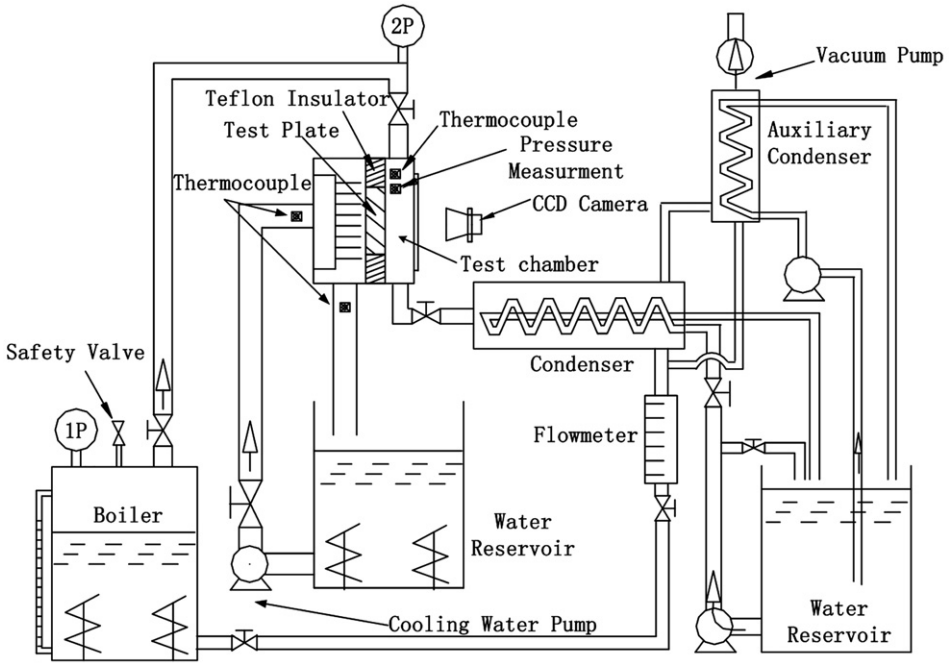

Fig. 1. Schematics of apparatus.

3. Method of measurement

3.1. Measurement of heat flux/transfer coefficient

To obtain surface temperature difference, an oblique block made of copper was constructed as shown in Fig. 2. The test block was fixed at the test chamber with Teflon to insulate from test chamber.

Details of thermocouple distribution and calculation for the test block were shown in Fig. 3. Twenty-four thermocouple holes, 0.5 mm dia., were drilled vertically at the cross section of the test block. Forty-five dots were added in the cross section of the test block to improve calculating accuracy. All thermocouples including measuring vapor temperature were calibrated against a platinum resistance thermometer in a high precision constant temperature bath.

The experimental process could be treated as a two-dimensional, quasi-steady state with no heat generation because of slow heating. Diagram for calculation was showed in Fig. 3; the open circle (○) corresponded to the thermocouple location, where the temperature could be measured. The closed circles (●) corresponded to insertion dot, where the temperature was obtained by calculation. These solid dots were all midpoint either between hollow/solid dots or between hollow/solid dot and surface. Calculation was performed using the following procedure:

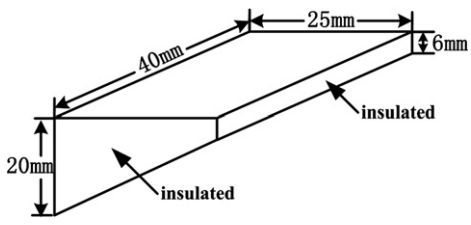

Fig. 2. Schematics of test block.

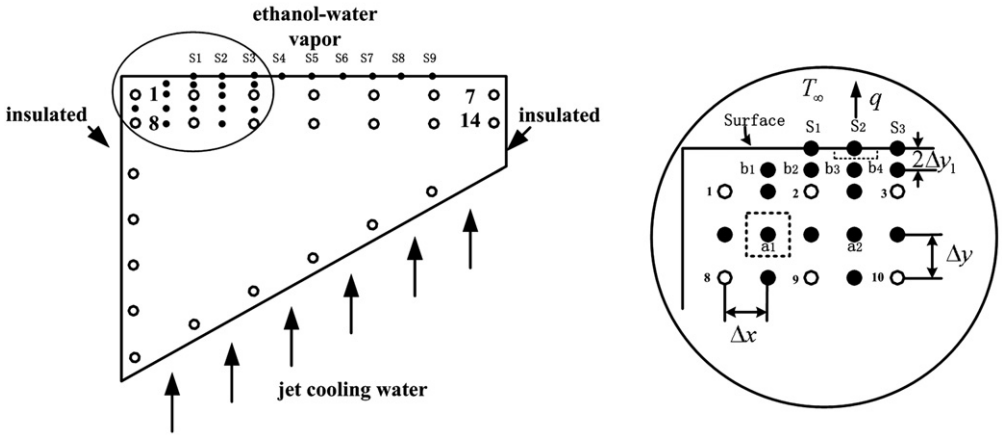

Fig. 3. Schematics of thermocouple distribution and enlargement of the ellipse in left.

Values of T_{8-9}, T_{9-10}, T_{1-8}, T_{2-9}, T_{1-2}, T_{3-10}, T_{2-3} were calculated by linear interpolation method. The values of these temperature above would be revised subsequently except T_{8-9}, T_{9-10}, T_{1-8}.

Considered the boundary shown in Fig. 3, the energy balance on node ($a1$) was

$$T_{a1} = \frac{(T_{1-8} + T_{2-9})\Delta y^2 + (T_{1-2} + T_{8-9})\Delta x^2}{2(\Delta x^2 + \Delta y^2)} \tag{1}$$

According to the same method, T_{a2} could be calculated. After getting T_{a1} and T_{a2}, the value of T_{29} could be revised. Identical approach was used for other solid dots till we obtained the value of all dots.

The energy balance equation on node S2 was written

$$-\lambda\Delta x\frac{T_{S2} - T_{b3}}{\Delta y_1} - \lambda\frac{\Delta y_1}{2}\frac{T_{S2} - T_{S1}}{\Delta x} - \lambda\frac{\Delta y_1}{2}\frac{T_{S2} - T_{S3}}{\Delta x} = h\Delta x(T_{S2} - T_\infty) \tag{2}$$

where λ, h, T_∞ were thermal conductivity, heat transfer coefficient, and bulk vapor temperature, respectively.

The local heat transfer coefficient of point S2 was deduced from Eq. (2), and heat flux q could easily get when obtaining temperature distribution.

3.2. Measurement of vapor concentration and velocity

UNIFAC (UNIQUAC functional-group activity coefficients) which was derived from UNIQUAC model by Fredenlund et al. (1975) was used to determine the ethanol concentration of the vapor mixtures. Based on this model, a program was developed to calculate the vapor concentration from the liquid concentration under different vapor pressures. At vapor pressure of 6.7 kPa, the results of UNIFAC were compared with the experimental data by Gmehling (1978) in Table 1. The result of the UNIFAC was in good agreement with the experimental data except for the very low concentrations. It demonstrated that the program of UNIFAC method was reliable.

Latent heat method and flowmeter method were separately applied to measure vapor velocity and the difference between the results from these two methods was less than 5%.

3.3. Uncertainties analysis

The experimental data reduction scheme relied on accurate test measurement. The uncertainties, associated with raw measurement and the derived data, were analyzed by the method of Moffat (1982). The uncertainty of heat conductivity (λ) was 2%, the temperature (T) was 0.1 K, the distance error between two holes were

Table 1
The comparison of experimental data by Gmehling and results of UNIFAC

Liquid concentration (%)	(Experimental data by Gmehling)		(Results of UNIFAC)	
	Vapor concentration (%)	Temperature (°C)	Vapor concentration (%)	Temperature (°C)
0.064	0.3320	30.90	0.3992	30.13
0.086	0.4080	29.40	0.4453	28.99
0.111	0.4680	28.15	0.4818	28.07
0.142	0.5120	27.10	0.5137	27.26
0.379	0.6320	23.90	0.6318	24.56
0.478	0.6690	23.25	0.6718	23.90
0.78	0.8220	21.95	0.8228	22.48
0.885	0.8980	21.70	0.8946	22.24

2×10^{-5} m and that of the non-condensable air concentration was 6 ppm. The resultant uncertainties of heat flux (q) and heat transfer coefficient (h) were 4–18% and 4–19%, respectively.

4. Results and discussion

4.1. Observation of condensation mode

As shown in Fig. 4, condensation mode depended on ethanol concentration and vapor-to-surface temperature difference (ΔT). Six condensation modes were observed, including smooth film (SF), bulk-drop (BD), drop-streak (DS), drop (D), wavy-drop (WD) and streak (S). Not every condensation mode appeared in process of every run. For low condensation (0.5%, 1%) and high condensation (50%), smooth film could be observed in high vapor-to-surface temperature difference. Drop mode easily occurred at high condensation while bulk-drop was a usual condensation mode at 0.5%, 1% and 2%. Drop-streak and streak could occur almost at all concentrations in low vapor-to-surface temperature difference. In wide region of vapor-to-surface temperature, for low condensation vapor, bulk-drop was main condensation mode. Meanwhile, an interesting phenomena, which the movement of drop or streak biased from left to right (thick end to thin end), could be observed. During the condensation, the drop grew rapidly in size by sweeping up other drops in its path and leaved behind a cleaner area for fresh condensation to begin.

4.2. Comparison of experimental results and Nusselt analysis

For film condensation on a vertical block, a theoretical heat transfer coefficient was calculated from Nusselt's theory of condensation. Due to maximal temperature difference between point S2 and S8 along transversal surface, the two points were chosen for comparison, S5 was also taken into account. A comparison of heat transfer coefficient was shown in Fig. 5.

The figure illustrated that Nusselt analysis was the lowest and the heat transfer coefficient of S2, S5 and S8 increased in turn under the same vapor-to-surface temperature difference.

One likely reason for the discrepancy between Nusselt analysis and experiment was due to that steam velocity was not zero ($v = 2$ m/s). Another plausible scenario was surface temperature difference that brought about by the test block shape. This difference might create difference of surface tension and lead to motion of molecules in condensation film. The movement of molecules would decrease heat resistance of condensation film. Further discussions were given in Sections 4.3 and 4.4.

4.3. Effect of surface temperature difference on heat flux

Owing to surface temperature gradient, it would influence heat flux distribution.

Fig. 6 showed temperature difference ($T_{S2} - T_{S8}$) and heat flux (q_{S2}, q_{S8}) were in terms of cooling water temperature (T_{cw}) under three experiment conditions.

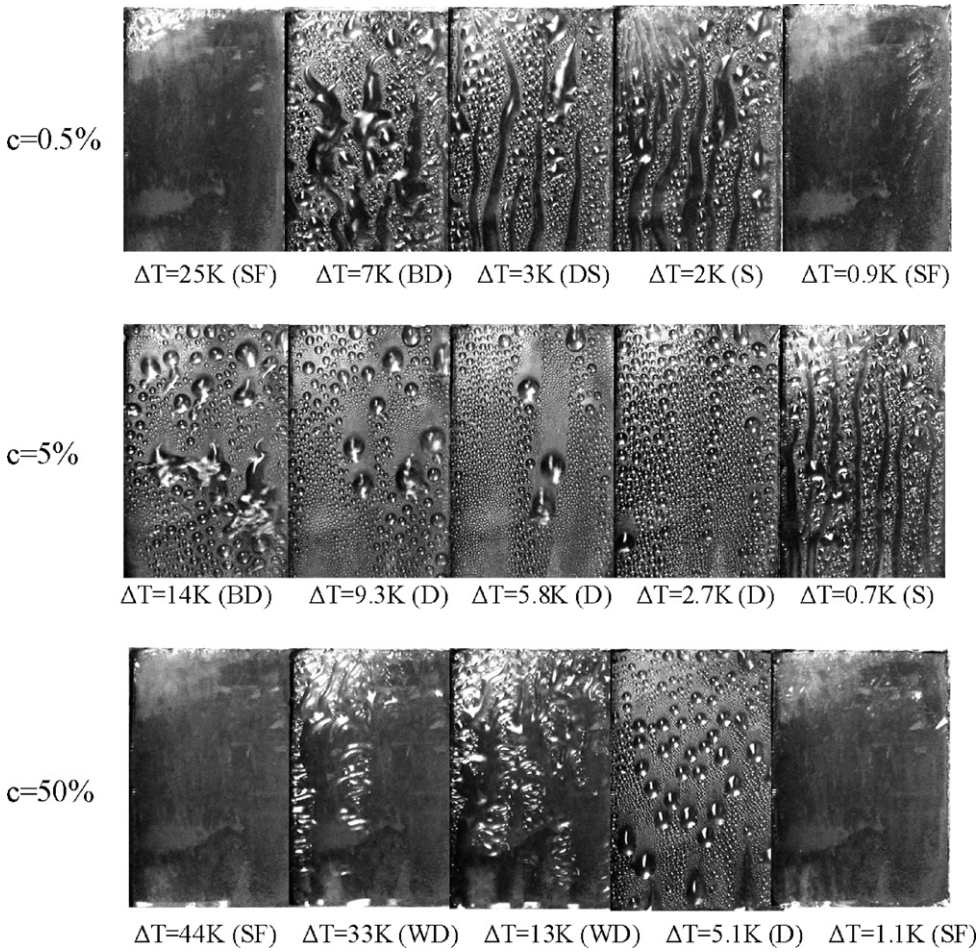

Fig. 4. Different condensation modes for different concentration ($v = 2$ m/s, $p = 84.5$ kPa) (condensation mode: SF, smooth film; BD, bulk-drop; DS, drop-streak; S, streak; D, drop; WD, wavy-drop).

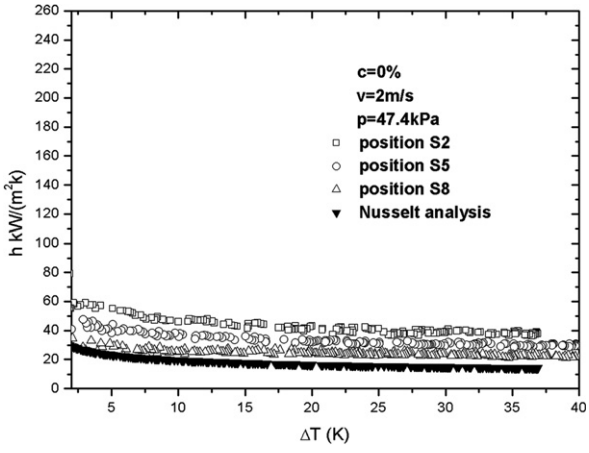

Fig. 5. Theory and experimental value.

As could be seen in Fig. 6, with increasing cooling water temperature, the temperature difference between S2 and S8 progressively decreased and trended to zero at last, this rule was applicable to all the concentrations

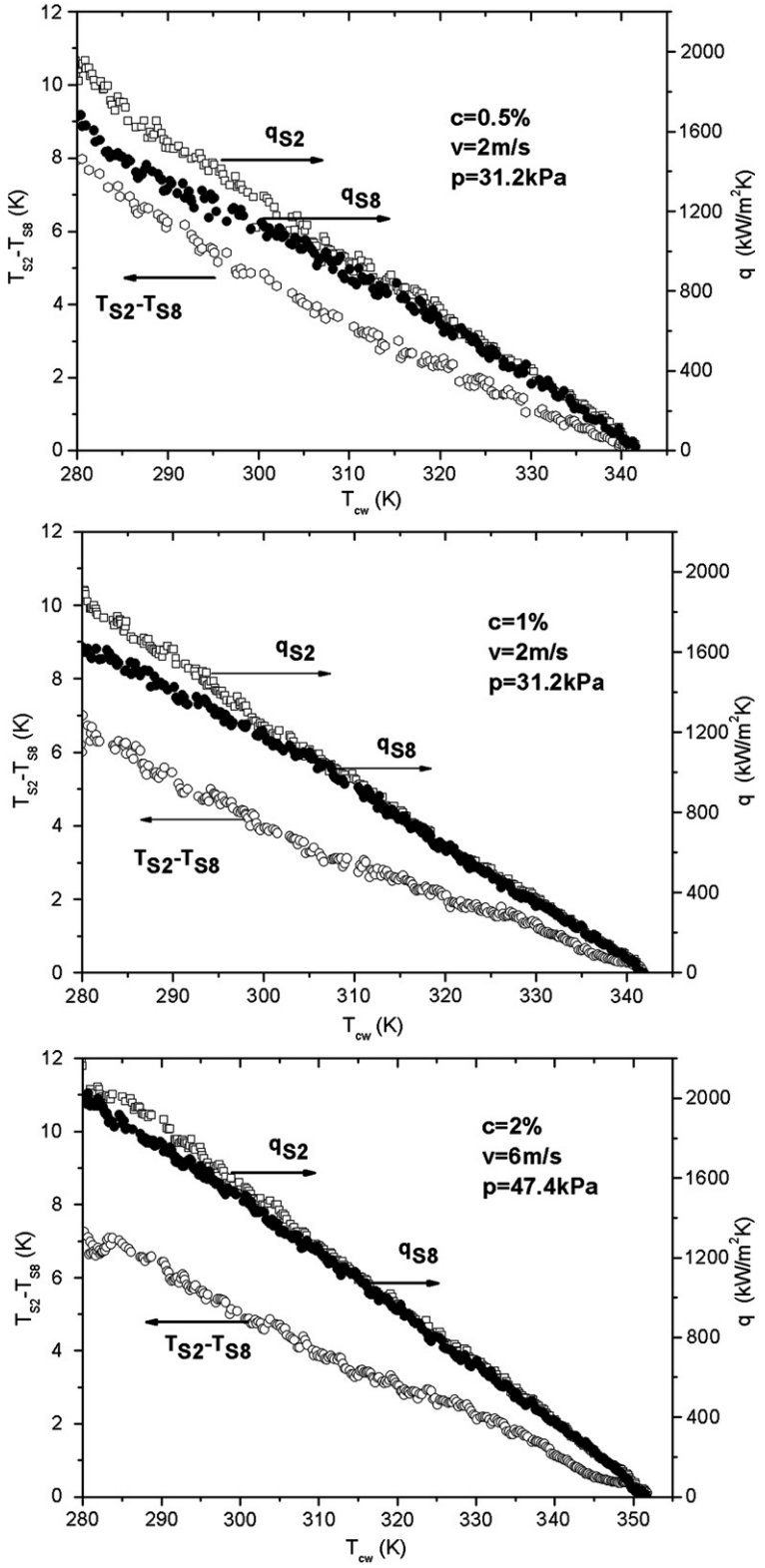

Fig. 6. Temperature difference between S2 and S8 ($T_{S2} - T_{S8}$) and heat flux (q_{S2}, q_{S8}) versus cooling water temperature (T_{cw}).

and velocities. When vapor velocity was relatively low ($v < 4$ m/s), the distinction of heat flux for S2 and S8 was obvious in high surface temperature difference (>4 K). While for high velocity ($v = 6$ m/s), although the surface temperature still existed, distinction of the two heat fluxes was less than that of fluxes at low velocity ($v < 4$ m/s) under identical cooling water temperature. In other words, the great magnitude of surface temperature played an important role for low velocity; the effect was moderated, however, by the increasing velocity of the vapor mixture for high velocity. For pure water, local heat flux at different position along the condensation surface was also various; the value at position S2 was greater than that at S8 as shown in Fig. 7.

The results given in both Figs. 6 and 7 could be combined to show that there existed various heat flux at difference position along the block surface due to surface temperature difference, and high surface temperature had great heat flux. A discrepancy in heat flux might be attributed to different thickness in condensation film, that is, surface region having a lower temperature accumulated more condensation film, and a thicker film showed greater heat resistance.

Two possible interpretations that created thickness difference might be considered:

- A first possible interpretation might be associated with the fact that, as vapor temperature kept constant, meaning that difference between vapor temperature and surface temperature for low temperature region (such as S8) was greater than that for high temperature region (such as S2). Higher difference temperature created a larger driving potential for condensation. Hence, more condensate accumulated in low temperature region.
- A second explanation might be concerned with surface tension variation due to surface temperature difference.

For ethanol–water mixtures, the surface tension was a function of concentration (c) and temperature (T), but the exact form of $\sigma(c, T)$ was beyond our knowledge; we only knew independently the dependence on the temperature $\sigma(c_0, T)$ at a fixed concentration and the dependence on the condensation $\sigma(c, T_0)$ at a fixed temperature.

For pure water, equilibrium surface tension dependence was well fitted by an expression:

$$\sigma(c, T) = -0.165(T - 273) + 75.97 \tag{3}$$

For an isothermal solution at uniform temperature T, surface tension dependence on concentration was given by a logarithmic law,

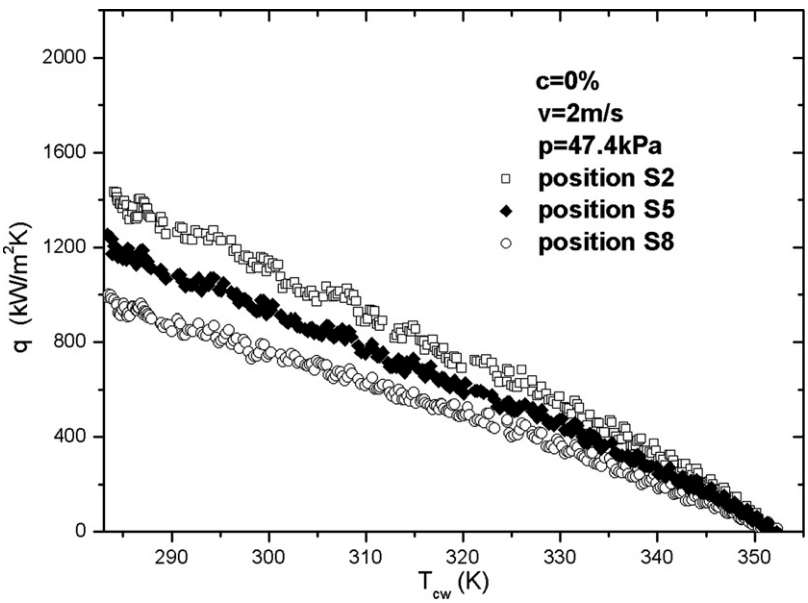

Fig. 7. Heat flux versus T_{cw} for S2, S5, and S8 ($c = 0\%$, $v = 2$ m/s, $p = 47.4$ kPa).

$$\sigma(c,T) = \sigma_0 - \sigma_0 b \ln\left(1 + \frac{c}{a}\right) \tag{4}$$

where $\sigma_0 = \sigma(0, T)$, a, b were undetermined constants, respectively.

The two undetermined constants a, b were found through experimental data recorded by Liu and Ma (2002), then expression (4) taken the form

$$\sigma = [-0.1649(T - 273) + 75.973]\left[1 - 0.411 \ln\left(1 + \frac{c}{1.37}\right)\right] \tag{5}$$

Table 2 given the values of experimental data, calculation data and error for different concentrations and temperature. As we could see, The values calculated using expression (5) were in good agreement (error $< \pm 1\%$) with the experimental values within our discussion. It demonstrated that the fitted expression (5) was feasible.

In order to observe variation of surface tension along the block surface, surface tension using fitted expression (5) to calculate versus cooling water temperature for S2, S5, and S8 was plotted as shown in Fig. 8(left). The same relation for pure water was also shown in Fig. 8(right). Average temperature of vapor temperature and local surface temperature was chosen to calculate surface tension. As could be seen in Fig. 8, with increase in cooling water temperature, surface tension gradually decreased, and it was owing to existence of temperature difference, distinct positions in oblique block had different surface tension under the same cooling water temperature, minimum and maximum values of surface tension lied in position S2 and S8, respectively.

Pure steam condensed on block surface and formed filmwise. For dropwise of ethanol–water mixtures, according to mechanism of dropwise condensation (Song et al., 1991), which a thin film of condensation existed on the area among the droplets and a thin film of condensate still existed at the spots of droplet departure. Thickness of condensation film varied inversely with the shape of the oblique block because of the rule of

Table 2
The comparison of experimental data in Liu and Ma (2002) and results of calculation

Liquid concentration (%)	Temperature (K)	Experimental data (mN/m)	Results of calculation (mN/m)	Error (%)
0.25/0.5/1	313	67.6/65.3/63	67.3/65.5/62.6	−0.44/0.34/−0.65
0.25/0.5/1	323	65.9/63.9/61.5	65.7/64.0/61.1	−0.30/0.10/−0.65
0.25/0.5/1	333	64.1/62.2/60	64.1/62.4/59.6	0.003/0.33/−0.64
0.25/0.5/1	343	62.6/60.8/58.7	62.5/60.9/58.1	−0.15/0.08/−0.98
0.25/0.5/1	353	60.9/59.1/57.1	60.9/59.3/56.6	0.004/0.33/−0.81
0.25/0.5/1	363	59.1/57.6/55.7	59.3/57.7/55.1	0.34/0.24/−0.98

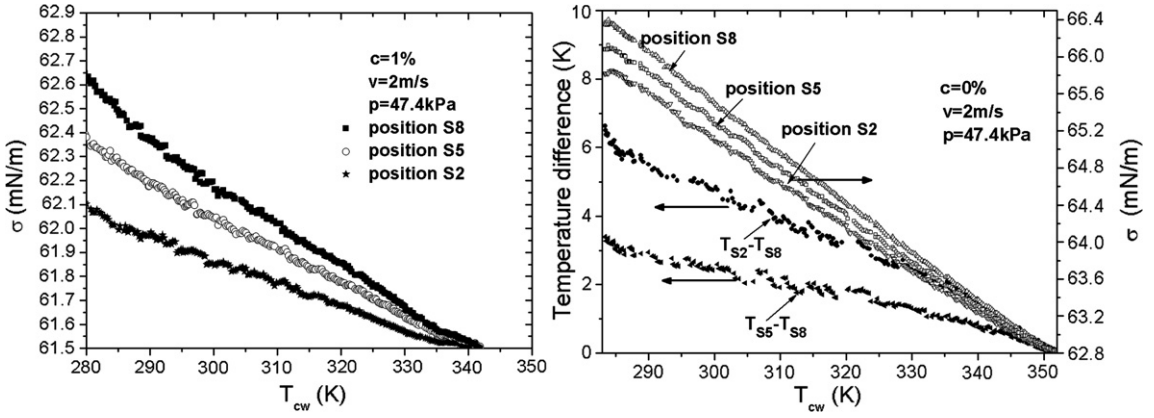

Fig. 8. Surface tension versus T_{cw} for S2, S5, S8 ($c = 1\%$, $v = 2$ m/s, $p = 47.4$ kPa) (left). Temperature difference (TS2–TS8, TS5–TS8) and surface tension versus T_{cw} for S2, S5, and S8 ($c = 0\%$, $v = 2$ m/s, $p = 47.4$ kPa) (right).

surface tension distribution. Such an interpretation was possible that, as condensation film became thin, it showed smaller heat resistance, enhancing heat flux due to heat resistance decreasing. The conclusion was in agreement with the experimental results that the heat flux of position S2 was greater than that of position S8.

4.4. Effect of vapor concentration on heat transfer

During experiment, heat transfer coefficient and vapor-to-surface temperature difference were diverse along the condensation surface of oblique block, a mean heat-transfer coefficient was introduced for the sake of comparison, and could be expressed as

$$\bar{h} = \frac{\bar{q}}{\overline{\Delta T}} = \frac{\int_0^L q\,\mathrm{d}x}{\int_0^L \Delta T\,\mathrm{d}x} \tag{6}$$

Where $\bar{h}$, $\bar{q}$, $\overline{\Delta T}$, L were mean heat transfer coefficient, mean heat flux, mean temperature difference, and length of surface, respectively. In the following sections, heat-transfer coefficient and vapor-to-surface temperature all referred to mean values.

The experiments were carried out for eight different concentrations of 0%, 0.5%, 1%, 2%, 5%, 10%, 20% and 50%, and results were provided in Fig. 9. It showed the characteristic curves of the tests under the fixed vapor pressure (84.5 kPa) and velocity (2 m/s) for a wide range of vapor concentrations.

For the case when ethanol condensation was low (0.5%, 1%), heat transfer coefficient gradually decreased with increasing vapor-to-surface temperature difference. As the vapor-to-surface temperature difference was progressively increased, the heat transfer coefficient at first increased, passed through a maximum and decreased subsequently for high concentration ethanol vapor mixtures ($c > 1\%$). When the ethanol concentration reached 50%, heat transfer coefficient was less than that of pure steam. For other velocities (4 m/s, 6 m/s) and other pressures (31.2 kPa, 47.4 kPa) (data not shown), variation tendency of characteristic curves was similar to Fig. 9. The maximum heat transfer coefficient (about 210 kW/m^{2}k) in the condensation characteristic curves appeared at an ethanol vapor mass fraction of approximately 1%. The experimental result was consistent with Utaka's (the maximum heat transfer coefficient was 180 kW/m^2 K, concentration was 1%), and shown in Fig. 9.

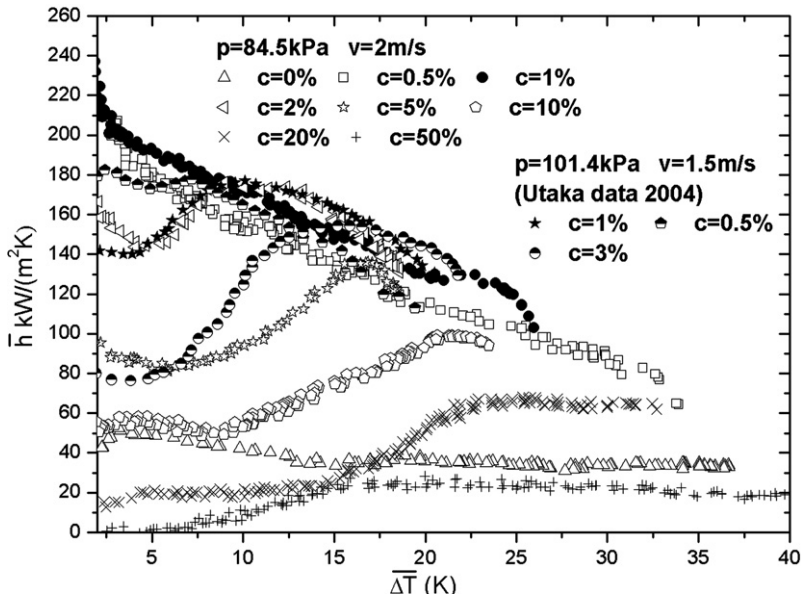

Fig. 9. Condensation heat transfer characteristic curves ($v = 2$ m/s, $p = 84.5$ kPa).

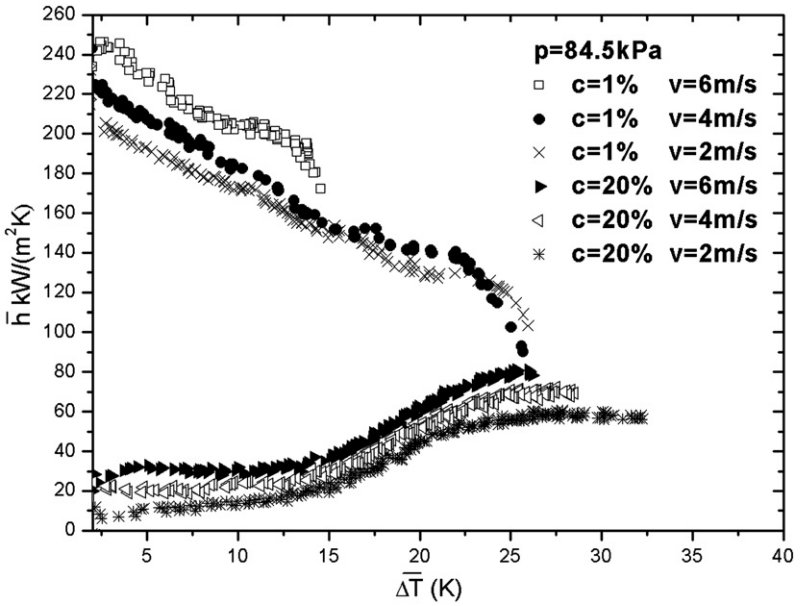

Fig. 10. Heat transfer coefficient versus vapor-to-surface temperature difference at various velocities.

The enhancement in heat transfer coefficient was due to surface tension difference, which induced by surface temperature difference. A surface tension gradient caused the convection flows and leaded to a substantial increase in heat (and/or mass) transfer rate. The molecules of the surface liquid layer were moved from the low surface tension region to the high one and dragged by viscosity the underlying liquid. This molecules motion could decrease film heat resistance and enhance heat transfer.

4.5. Effect of vapor velocity on heat transfer

For vapor mixtures, the heat transfer coefficients increased with the vapor velocity as shown in Fig. 10. It could be conclude that the increasing of vapor velocity led to increasing of vapor mass velocity and condensate flux, and enhanced the disorder between condensate and vapor, correspondingly the thermal resistance in condensate and diffusion resistance in vapor-side were decreased, and accordingly the condensation heat transfer coefficient was augmented.

4.6. Effect of vapor pressure on heat transfer

In our study, experiments were conducted at three pressures, namely 31.2 kPa, 47.4 kPa and 84.5 kPa. The results generally demonstrated that the heat transfer coefficients of all vapors increased with pressure, no matter it was steam or vapor mixtures. Fig. 11 showed the condensation characteristic curves of different pressures at two ethanol concentrations of 1% and 10% ($v = 2$ m/s).

5. Conclusions

In this work, the influence of the macroscopic temperature gradient on the heat transfer coefficient has been studied at varied pressure and velocity of the vapor mixtures under a wide range of concentrations. The results showed that macroscopic temperature gradient caused both difference of local heat flux and a higher mean heat transfer, compared with that without temperature gradient. In the studied ranges, the results have shown that:

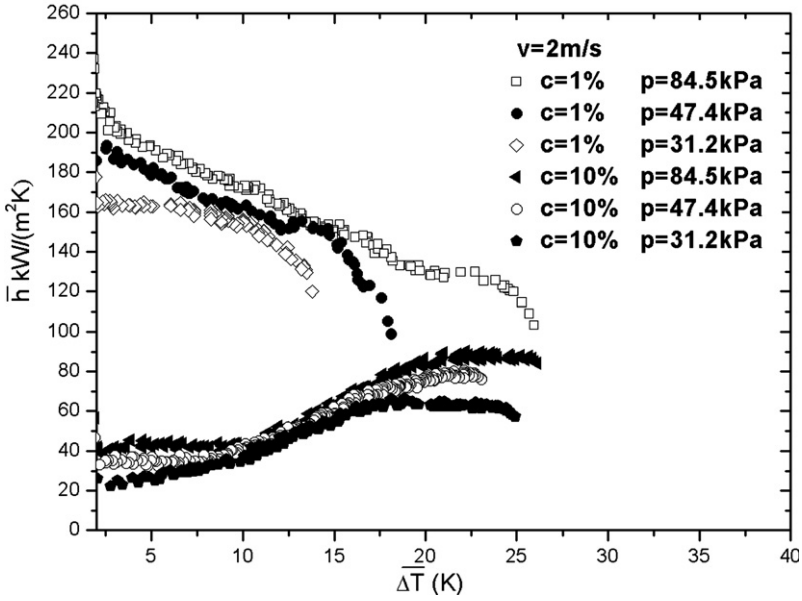

Fig. 11. Heat transfer coefficient versus vapor-to-surface temperature difference at various pressures.

- Owing to surface temperature difference, heat flux and surface tension were varied along the condensation surface at the same cooling water temperature. Difference in heat transfer and surface tension between two ends of the oblique block was greatest along the surface at low velocity ($v < 4$ m/s). Variation in local heat flux might be attributed to the discrepancy of condensation liquid film thickness along the surface and difference of condensation rate.
- The maximum mean heat transfer coefficient, which was greater than the value presented in literature under similar experimental conditions, appeared at an ethanol vapor concentration about 1%. The enhancement possible had recourse to the surface temperature difference and caused the convection flows, leading to a substantial increase in heat (and/or mass) transfer rate. A further increase in ethanol concentration decreased the heat transfer coefficient.
- For steam and various concentration ethanol–water mixtures, with increasing velocity and pressure, the heat transfer coefficient increased.

However, much more careful study may be necessary to understand the detailed mechanisms in the future study.

Acknowledgement

This project has been supported by National Natural Science Foundation of China through Grant Nos.50476048 and 50521604.

References

Chris, P., Joe, D., 2004. The condensation of ammonia–water mixtures in a horizontal shell and tube condenser. J. Heat Transf. 126, 527–534.

Ford, J.D., Missen, R.W., 1968. On the conditions for stability of falling films subject to surface tension disturbances; the condensation of binary vapors. Can. J. Chem. Eng. 48, 309–312.

Fredenlund, A., Jones, R.L., Prausnitz, J.M., 1975. Group contribution estimation of activity coefficients in non-ideal liquid mixtures. AIChEJ 27, 1086–1099.

Fujii, T., Koyama, S., Shimizu, Y., Watabe, M., Nakam-ura, Y., 1989. Gravity controlled condensation of an ethanol and water mixture on a horizontal tube. Trans. Jpn. Soc. Mech. Eng. (Ser. B) 55, 210–215.

Fujii, T., Osa, N., Koyama, S., 1993. Free convection condensation of binary vapor mixtures on a smooth horizontal tube: condensing mode and heat transfer coefficient of condensate. In: Proc. US Eng. Found. Conf., pp. 171–182.

Gmehling, J., 1978. Vapor–liquid equilibrium data collection: organic hydroxyl compounds: alcohol and phenols. Chemistry Data Series, vol. 1, Part 2a, Frankfurt.

Hijikata, K., Nakabeppu, O., Fukasaku, Y., 1992. Condensation characteristics of a water–ethanol binary vapor mixture. In: Proc. of 29th Japan Heat Transfer Symp., pp. 742–743.

Hijikata, K., Fukasaku, Y., Nakabeppu, O., 1996. Theoretical and experimental studies on the pseudo-dropwise condensation of a binary vapor mixture. J. Heat Transf. 118, 140–147.

Kim, J., Lefsaker, A.M., Razani, A., Stone, A., 2001. The effective use of heat transfer additives for steam condensation. Appl. Therm. Eng. 21, 1863–1874.

Liu, G.Q., Ma, L.X., 2002. Handbook of Chemical Engineering Calculations. Chemical Industry Press, Beijing.

Mirkovich, V.V., Missen, R.W., 1961. Non-filmwise condensation of binary vapors of miscible liquids. Can. J. Chem. Eng. 39, 86–87.

Mirkovich, V.V., Missen, R.W., 1963. A study of the condensation of binary vapors of miscible liquids II: heat transfer coefficients for filmwise and non-filmwise condensation. Can. J. Chem. Eng. 41, 73–78.

Moffat, R.J., 1982. Contributions to the theory of single-sample uncertainty analysis. J. Fluids Eng. Trans. ASME 104, 250–260.

Morrison, J.N.A., Deans, J., 1997. Augmentation of steam condensation heat transfer by addition of ammonia. Int. J. Heat Mass Transf. 40, 765–772.

Song, Y.J., Xu, D.Q., Lin, J.F., 1991. A study on the mechanism of dropwise condensation. Int. J. Heat Mass Transf. 34, 2827–2831.

Utaka, Y., Terachi, N., 1995. Study on condensation heat transfer for steam–ethanol vapor mixture (Relation between condensation characteristic curves and modes of condensate). Trans. Jpn. Soc. Mech. Eng. (Ser. B) 61, 3059–3065.

Utaka, Y., Terachi, N., 1996. Measurement of condensation characteristic curves for binary mixture of steam and ethanol vapor. Heat Transf.-Jpn Res. 24, 57–67.

Utaka, Y., Wang, S.X., 2004. Characteristic curves and the promotion effect of ethanol addition on steam condensation heat transfer. Int. J. Heat Mass Transf. 47, 4507–4516.

Yan, J.J., Yang, Y.S., Hu, S.H., Zhen, K.J., Liu, J.P., 2007. Effects of vapor pressure/velocity and concentration on condensation heat transfer for steam–ethanol vapor mixture. Heat Mass Transf., in press, doi:10.1007/S00231-006-0216-5.